Photoinduced DNA Cleavage and Cellular Damage in Human Dermal Fibroblasts by 2,3-Diaminophenazine

Author(s): Patty K-L. Fu, Sonia Abuzakhm, Claudia Turro
Source: Photochemistry and Photobiology, 81(1):89-95.
Published By: American Society for Photobiology
DOI: http://dx.doi.org/10.1562/2004-07-20-RA-237.1
URL: http://www.bioone.org/doi/full/10.1562/2004-07-20-RA-237.1

Photochemistry and Photobiology, 2005, 81: 89–95

Photoinduced DNA Cleavage and Cellular Damage in Human Dermal Fibroblasts by 2,3-Diaminophenazine¶

Patty K.-L. Fu*[1], Sonia Abuzakhm[2] and Claudia Turro*[2]

[1]Center for Food Safety and Applied Nutrition, U.S. Food and Drug Administration, College Park, MD
[2]Department of Chemistry, The Ohio State University, Columbus, OH

Received 20 July 2004; accepted 7 October 2004

ABSTRACT

Aromatic amines, such as *o*-phenylenediamine (OPD), have been used extensively in commercial hair dyes and in the synthesis of agricultural pesticides. Air oxidation of OPD results in the formation of 2,3-diaminophenazine (DAP). Although the mutagenic toxicity of DAP has been shown in both prokaryotic and eukaryotic systems, its phototoxicity remains largely unexplored. This study focuses on the pH-dependent photophysical properties of DAP and demonstrates its ability to photoinduce DNA damage to pUC19 plasmid *in vitro*. The photocytotoxicity of DAP toward human skin fibroblasts was also measured. DAP exhibits weak intercalative binding to double-stranded DNA with a binding constant $K_b = 3.5 \times 10^3\ M^{-1}$. Furthermore, upon irradiation with visible light, DAP is able to nick plasmid DNA in the presence of oxygen. The concentration of DAP that resulted in 50% cell death was 172 ± 9 μ*M* in the dark and 13 ± 1 μ*M* after irradiation of the DAP-treated cell cultures with visible light (400–700 nm, 30 min, 5 J/cm^2). The 13-fold increase in toxicity upon exposure to visible light shows the need for further study of the photocytotoxicity of contaminants such as DAP.

INTRODUCTION

Phenylenediamines, such as *o*-phenylenediamine (OPD), are the most common and widely used aromatic amines for the formulation of commercial hair dyes and synthesis of agricultural fungicides (1–4). In addition, OPD is one of the most effective chromogenic substrates for a variety of enzyme-linked immunosorbent assays (ELISA) used in the study of enzyme kinetics (5–7). The use of OPD in the ELISA assays permits the use of spectrofluorometric detection, which results in a significant increase in sensitivity (5–7).

Two toxic byproducts formed upon routine handling of OPD are 2,3-diaminophenazine (DAP) and 2-amino-3-hydroxyphenazine (AHP) (1–13). DAP is considered to be the major mutagenic contaminant generated from the oxidation of OPD (Fig. 1), which can be carried out by oxygen in air and is accelerated by exposure to light (1–15). AHP results from a chemical transformation of DAP in aqueous media (12,13). Both DAP and AHP are well-recognized toxic environmental contaminants and industrial occupational hazards (1,2,4,12,13). The mutagenic effects and the genotoxicity of DAP and AHP have been reported in both prokaryotic and eukaryotic systems (12–14), and it has been shown that DAP induces chromosomal DNA damage in bacteria, human blood lymphocytes and mice (1,2,12–15).

The photophysical properties of DAP remain largely unexplored, although the molecule is known to be highly emissive (5–7,16–22). Most investigations of DAP fluorescence have typically focused on its use in the development of new analytical applications and detection techniques (5–7,16–22); however, the potential biological impact of its excited-state photochemistry remains unknown. Because genotoxicity tests to date have focused on the ground-state reactivity (1–4,12–15) and were, therefore, carried out in the absence of irradiation, the photobiological effects and the phototoxicity of DAP are not well understood. Because of the potential human exposure to DAP generated from the oxidation of OPD in topically applied hair dyes, it is important to further examine the excited-state properties and reactivity of DAP toward biomolecules. In this study, we explore the photophysical and photochemical properties of DAP, as well as its ability to sensitize light-induced DNA cleavage in plasmid, and cellular damage in human skin fibroblasts.

MATERIALS AND METHODS

Materials and chemicals. $FeCl_3$, OPD, HCl, D_2O, ethylenediaminetetraacetic acid (EDTA) and formamide were purchased from Aldrich (St. Louis, MO). Ethidium bromide (EtBr), NaCl, calf thymus DNA (CT DNA), dialysis membrane (>100 000 Da), Tris–acetate EDTA (TAE) buffer, Na_2HPO_4, NaH_2PO_4, agrose, *N*-lauroyl sarcosine, micro-Lowry reagent kit 690-A and Folin–Ciocalteau phenol reagent were purchased from Sigma (St. Louis, MO). Sonicated herring sperm DNA purchased from Promega (Madison, WI). pUC19 plasmid and gel loading solution were purchased from New England Biolabs (Beverly, MA). Dulbecco modified Eagle media, fetal bovine serum, phosphate-buffered saline (PBS), gentamicin, glucose, L-glutamine were purchased from Invitrogen Corp (Carlsbad, CA).

Synthesis. DAP was synthesized from $FeCl_3$ and OPD according to a reported method (23). $FeCl_3$ (0.7120 g) was dissolved in 20 mL of H_2O

¶Posted on the website on 19 October 2004.

*To whom correspondence should be addressed (PKF) at: Center for Food Safety and Applied Nutrition, U.S. Food and Drug Administration, 5100 Paint Branch Parkway, College Park, MD 20740, USA. Fax: 301-436-2897; e-mail: patty.fu@FDA.GOV

*To whom correspondence should be addressed (CT) at: Department of Chemistry, The Ohio State University, Columbus, OH 43210, USA. Fax: 614-292-1685; e-mail: turro@chemistry.ohio-state.edu

Abbreviations: AHP, 2-amino-3-hydroxyphenazine; CT DNA, calf thymus DNA; DAP, 2,3-diaminophenazine; ds-DNA, double-stranded DNA; EDTA, ethylenediaminetetraacetic acid; ELISA, enzyme-linked immunosorbent assay; EtBr, ethidium bromide; ^{1}H NMR, proton nuclear magnetic resonance; LC_{50}, lethal concentration 50; OPD, *o*-phenylenediamine; PBS, phosphate-buffered saline; TAE, Tris–acetate.

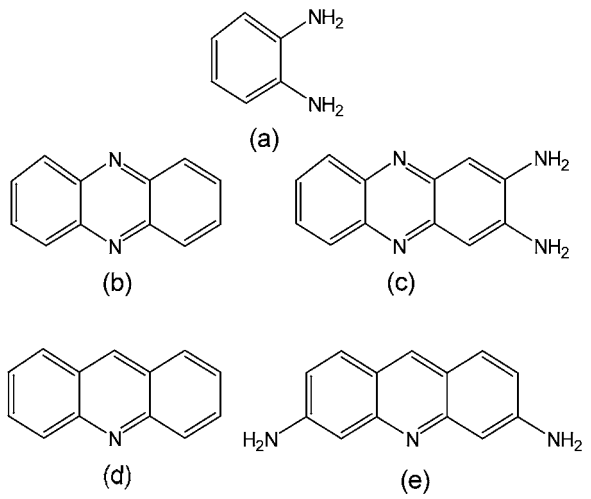

Figure 1. Structure of (a) OPD, (b) phenazine, (c) DAP, (d) acridine ring and (e) proflavin.

and was poured into a stirring solution containing OPD (0.2160 g) and 20 mL of HCl in 0.6 mL H_2O at room temperature. The red precipitate was filtered and washed repeatedly with diethylether and methanol. Proton nuclear magnetic resonance (^{1}H NMR) (400 MHz, D_2O): $\delta = 8.0$ (m, 2H); 7.7 (m, 2H); 6.9 (s, 2H); 6.2 (s, 4H). The ^{1}H NMR spectrum of the product in D_2O was consistent with that reported previously for DAP (23).

Absorption, fluorescence and irradiation source. Absorption measurements were performed using a Hewlett Packard diode array spectrometer (HP8453) with HP8453Win System software installed on an HP Vectra XM 5/120 desktop computer (Loveland, CO). Emission spectra for the pH titrations were collected using a SPEX FluoroMax-2 spectrometer (Edison, NJ) equipped with a 150 W Xenon source, a red-sensitive 928P photomultiplier tube and DataMax-Std software on a Pentium microprocessor. The emission experiments in the presence of DNA (pH = 7.5 with λ_{exc} = 430 nm and λ_{em} = 590 nm) were carried out using a MFX fluorimeter (Dynex Technology, Chantilly, VA) using Revelation software on a Micron PC. The source of visible radiation (400–700 nm) for DNA photocleavage and photocytotoxicity was a photoreactor (Luzchem, Ontario, Canada) composed of twelve 8 W GE watt-miser bulbs (Luzchem). The light intensity was measured using a radiometer (International Light Inc., Newburyport, MA).

Equilibrium dialysis. CT DNA was purchased from Sigma and purified using a standard literature procedure (24). First, the same volume of formamide denaturing buffer (20 m*M* Tris–HCl, pH 8.0, 0.8 *M* NaCl, 80% vol/vol formamide) was added to the CT DNA solution (1 mg/mL) and left for 12 h at 15°C, which results in the denaturation of any proteins bound to CT DNA. After the incubation, the solution was dialyzed using >100 000 Da dialysis membrane (Sigma) for 45 min against 1 L of a buffer containing 20 m*M* phosphate buffer (pH = 8.0), 0.1 *M* NaCl and 10 m*M* EDTA; the buffer was replaced and the dialysis repeated three times in 4 h intervals. The CT DNA was then dialyzed twice against 10 m*M* phosphate buffer (pH 8.0), 10 m*M* NaCl, 0.5 m*M* EDTA for 8–10 h. The dialysis membrane was prepared according to standard methods (24). The 10–20 cm long pieces of tubing were boiled for 10 min in ~500 mL of 2% (wt/vol) sodium bicarbonate and 1 m*M* EDTA (pH = 8.0),were then rinsed thoroughly with deionized H_2O and were then boiled for 10 min in 1 m*M* EDTA and allowed to cool. The tubes were stored at 4°C submerged in 1 m*M* EDTA and were rinsed thoroughly with deionized H_2O before use.

In the binding constant determination using dialysis, the total concentration of DAP (C_t) present in the dialysate solution was determined spectrophotometrically using an extinction coefficient, ε, of 13 000 cm^{-1} M^{-1} at 440 nm. The exctinction coefficent was measured using Beer's Law. CT DNA (100 μ*M*) was placed in a dialysis membrane and was dialyzed against 1.0 L of 10 μ*M* DAP in circulating buffer (6 m*M* Na_2HPO_4, 3 m*M* NaH_2PO_4, 1 m*M* EDTA and 125 m*M* NaCl, pH = 7.0) for 48 h. The free DAP concentration (C_f) was determined from an aliquot of the dialysate solution after the 48 h equilibration period. The amount of DAP bound to the CT DNA, C_b, was determined from the mass balance equation given by $C_b = C_t - C_f$ (25–27).

Spectrophotometric titration. The binding constant of DAP to CT DNA was determined by absorption titration at room temperature using 10 individual freshly prepared solutions with a constant concentration of DAP (25 μ*M*) and CT DNA concentrations that ranged from 0 to 125 μ*M* (5 m*M* NaCl, 10 m*M* phosphate buffer, pH 7.5). The binding constant, K_b, was determined from the absorption changes during the DNA titration and was calculated using the equation $(\varepsilon_a - \varepsilon_b)/(\varepsilon_b - \varepsilon_f) = (1/K_b) \times (1/[DNA]) + 1$, where ε_a, ε_f and ε_b are the molar extinction coefficients for the apparent absorption of the complex at a given DNA concentration, for the complex free in solution and for the complex fully bound to DNA, respectively. The value of ε_b was determined from the titration where further addition of DNA did not result in changes to the spectrum. The binding constant for each molecule was determined by plotting $(\varepsilon_a - \varepsilon_b)/(\varepsilon_b - \varepsilon_f)$ *vs* 1/[DNA], and K_b was obtained as the reciprocal value of the slope (28,29).

Viscosity measurements. The viscosity experiments were performed using a Cannon-Manning semi-micro size 75 viscometer (State College, PA) immersed in a thermostated water bath maintained at 25°C (±0.1). Solutions (1 mL 25 m*M* phosphate buffer, pH = 7.2) containing 2.5 m*M* (base pairs) sonicated herring sperm DNA purchased from Promega and used without further purification. Titrations were conducted by the successive addition of either EtBr or DAP directly into the viscometer without removing the DNA solution, and the solutions were bubbled with nitrogen after each addition to ensure mixing (30–32). The data points were plotted as $(\eta/\eta_0)^{1/3}$ *vs* [Compound]/[DNA bp], where η_0 and η represent the viscosity of the DNA solution in the absence and presence of a given compound, respectively, both relative to the viscosity of the buffer at the same temperature (30–33). Both η and η_0 were calculated from the observed flow times, *t*, relative to the flow time for the buffer, t_0 (98.5 ± 0.5 s). The flow time of DNA alone was measured to be 140.2 ± 0.5 s at 25°C.

DNA photocleavage. The DNA photocleavage experiments were carried out on a 20 μL total sample volume in 0.5 mL transparent eppendorf microtubes containing 120 μ*M* pUC19 plasmid and 30 μ*M* of DAP in 10 m*M* phosphate buffer, 5 m*M* NaCl, pH = 7.5. All samples were irradiated for 30 min after 30 min of incubation following addition of DAP. After irradiation, the samples were loaded into the gel following the addition of 4 μL of DNA gel loading solution to each reaction mixture. In determining the pH dependence of photocleavage, the pH of each reaction mixture was varied using phosphate buffer before adding DAP and irradiation. All the photolysis experiments were conducted in air at room temperature. The electrophoresis was carried out using 2% agarose gel stained with 0.5 mg/L EtBr in 1× TAE running buffer at 90 V for 1.5 h and the gels were imaged on a GelDoc 2000 transilluminator (Bio-Rad, Hercules, CA). The extent of photocleavage was calculated from the ratio of nicked (circular) to supercoiled double-stranded DNA (ds-DNA) determined from the integration of image intensity available in the QuantityOne Analysis System software (Bio-Rad). In these measurements, no correction was made for the difference in EtBr emission from the different forms of DNA.

Cytotoxicity and photocytotoxicity assays. Human skin fibroblasts (Hs-27) were obtained from the American Type Culture Collection, cell line CRL-1634 (Manassas, VA). The cells were cultured in Dulbecco modified Eagle media, containing 10% fetal bovine serum, 50 μg/mL gentamicin, 4.5 mg/mL glucose and 4 m*M* L-glutamine. The cell cultures were incubated in a humidified atmosphere containing 5% CO_2 at 37°C.

For assessing the cytotoxicity and photocytotoxicity of DAP, >80% confluent monolayers of Hs-27 in 60 mm culture dishes were used. The monolayers were first washed twice with PBS to ensure that the culture dishes were free of any culture medium. Fresh PBS (3 mL) containing various concentrations of DAP was then added to cover the fibroblasts. The cells were irradiated through the PBS buffer, which does not absorb light in the visible region, immediately without an incubation period. The spectral output of the visible light was $\sim 2.8 \times 10^{-3}$ W/cm^2, and all samples were irradiated no longer than 30 min (~5 J/cm^2) at room temperature. After irradiation, the cells were removed from the dishes by trypsinization, reseeded into 24-well culture dishes and incubated for 48 h. *N*-lauroyl sarcosine (200 μL, 40 m*M*) was then added to each well and the cells were allowed to lyse for at least 30 min. Quantitative determination of the protein content in each well was undertaken using Peterson modification of the micro-Lowry method. The lysate was treated with 200 μL Lowry reagent for 30 min and then with 100 μL Folin–Ciocalteau phenol reagent for 30 min. A portion (200 μL) of the contents of each well was transferred to a 96-well plate for absorbance determination using a 96-well MRX plate reader (Dynatech Laboratory, DynPort, VA). The absorbance measured at 630 nm is proportional to the total protein content and the number of cells in each well.

RESULTS AND DISCUSSION

Photophysical properties in solution

The absorption spectrum of DAP in H_2O is characterized by a maximum at 420 nm ($\varepsilon = 13\,000\ M^{-1}\ cm^{-1}$), and excitation in the visible region (400–450 nm) results in emission with a maximum at 583 nm. Pronounced changes in the electronic absorption and emission spectra of DAP as a function of pH are observed and are shown in Fig. 2. The absorption maximum of DAP shifts from 450 to 417 nm as the pH is varied from 4.0 to 8.0 (Fig. 2a). Weak emission is observed at pH = 3.0 with a maximum at 575 nm, and a 13-fold increase in intensity is observed as the pH is raised to 9.0 with a shift in the maximum to 585 nm (Fig. 2b). The pH-dependent changes we observe in the absorption and the emission intensities result from two protonation steps at pH = 5 and pH = 6.6, agreeing with the previously published pk_a value of 5.1 (34). The changes in absorption and emission as a function of solution pH are indicative of the existence of ground-state species with different degrees of protonation, which possess different luminescence properties (35–44).

The pH and solvent dependence of the emission of various heterocyclic aromatic dyes, such as acridine, phenazine, proflavin (3,6-diaminoacridine) and their derivatives (Fig. 1) have been investigated previously (35,36,40). The redshift of the absorption maximum of DAP shown in Fig. 2a as the solution pH is decreased is similar to that observed in proflavin. This pH-dependent redshift was attributed to the protonation of proflavin's ring nitrogen with a pk_a = 9.5 (35,36). The protonation of the amino nitrogen in proflavin with pk_a values of 0.2 does not result in significant spectral changes (35,40). The protonation of the nitrogen in the aromatic ring of phenazine and acridine with pk_a values of 1.21 and 5.4, respectively, has also been reported to result in significant spectral changes both in the absorption and emission maxima (39,42,43). Because amination increases the basicity of the aromatic nitrogen in acridine, the amino substituents in DAP result in a shift in the pk_a value from 1.21 in phenazine to 5.1 for DAP. The magnitude of this shift is similar to that observed for protonation of the aromatic nitrogen between acridine (pk_a = 5.4) and proflavin (pk_a = 9.5). Therefore, it is likely that the observed spectral shifts and intensity changes in DAP are because of protonation of the nitrogens in the aromatic ring.

Previous study on the photophysical properties of phenazine, whose structure is shown in Fig. 1, reveals that it is a weak fluorophore, but it is strongly phosphorescent (41–44). The lowest energy singlet exited state, S_1, of D_{2h} phenazine is $^1B_{1u}$ ($n\pi^*$). It has been noted that there is a significant overlap of phenazine's $^1B_{1u}$ ($n\pi^*$) state with its $^3B_{3u}$ ($\pi\pi^*$) state, which is the lowest energy triplet excited state of the molecule, T_1. Because of this mixing of the $^1B_{1u}$ and $^3B_{3u}$ states, the intersystem crossing rate from S_1 to T_1 is much faster than the radiative decay from S_1 to the ground state, S_0 (41,42). However, incorporation of substituents such as amino groups, on the aromatic rings of phenazine, results in lowering of the $n\pi^*$ S_1 energy relative to $\pi\pi^*$ T_1, thus increasing the fluorescence quantum yield and shifting the emission and absorption maxima to lower energies (42,43). These results are consistent with the strong fluorescence observed for DAP.

DNA binding

The binding constant of DAP to ds-DNA was determined using both equilibrium dialysis and spectrophotometric titrations. To avoid polymerization because of exposure to low levels of ultraviolet–visible light (45–47), 10 individual solutions were freshly prepared with a constant concentration of DAP (25 μM) and ds-DNA concentrations that ranged from 0 to 125 μM. The absorption spectrum of 25 μM DAP showed a notable 20 ± 1% hypochromicity as ds-DNA concentration was increased to 125 μM, along with a small redshift of the absorption maximum (~3 nm). A binding constant $K_b = 2.5 \times 10^3\ M^{-1}$ was obtained using the changes in DAP absorption at 420 nm as a function of ds-DNA concentration at pH = 7.0 by methods reported previously (28,29,48–50). A slight decrease in K_b ($2.1 \times 10^3\ M^{-1}$) was observed when the spectrophotometric experiments were conducted at pH = 4.0, which is likely within the experimental error of the measurement.

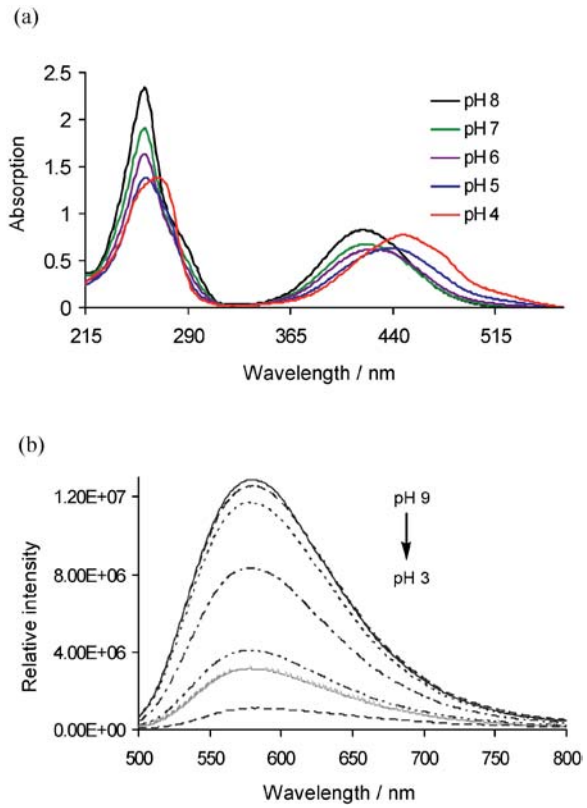

Figure 2. Room temperature (a) electronic absorption and (b) emission (λ_{exc} = 440 nm) spectra of DAP at different pH values.

The DNA binding constant for DAP, K_b, obtained from the equilibrium dialysis experiment was calculated from $K_b = C_b/[C_f(S_{total} - C_b)]$, where C_b and C_f are the concentrations of DAP bound to the DNA and free in solution after the dialysis, respectively, and S_{total} represents the total nucleic acid concentration (25–27,48–51). The total DAP and nucleic acid concentrations were 10 and 100 μM, respectively, which resulted in $K_b = 3.5 \times 10^3\ M^{-1}$. This value is in excellent agreement with that obtained from the spectrophotometric method. This low binding constant for DAP with ds-DNA is indicative of a weak interaction, although the extended π-system of DAP makes the molecule a good candidate for strong binding through intercalation. Common DNA intercalators such as EtBr, proflavin and daunomycin exhibit DNA binding constants $\sim 10^5\ M^{-1}$, which are ~100-fold greater than that of DAP (51–53).

As shown in Fig. 3a, after addition of ds-DNA to solutions containing 50 μM DAP (50 mM NaCl, 10 mM phosphorus buffer,

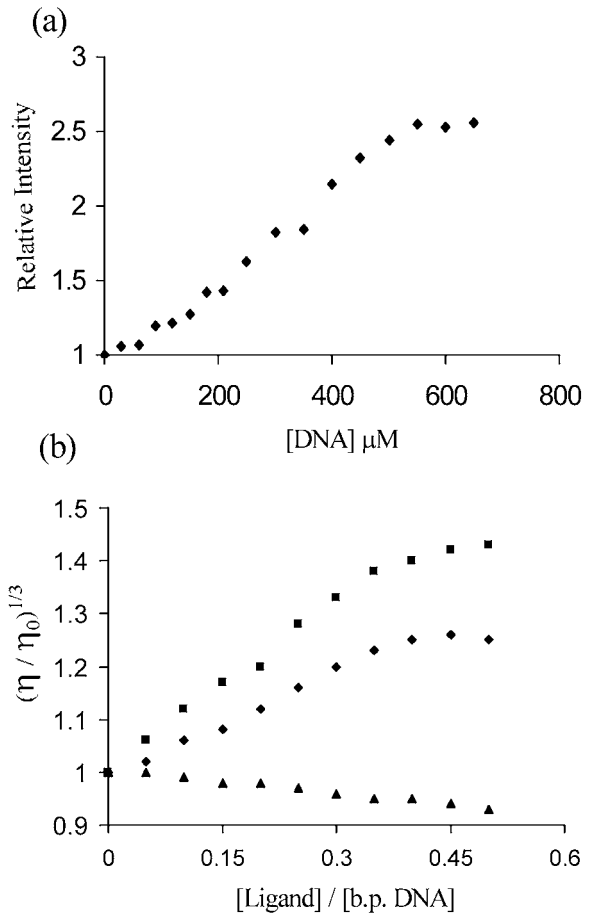

Figure 3. a: Relative emission of 50 μ*M* DAP (λ_{exc} = 430 nm, λ_{em} = 590 nm) in 50 m*M* NaCl, 10 m*M* phosphorus buffer, pH = 7.5, as a function of added CT DNA (5% error in reproducibility). b: Change in the relative viscosity of 2.5 m*M* sonicated herring sperm DNA solution with increasing concentration of EtBr (■), DAP (◆) and Hoechst 33258 (▲). A low-salt buffer (25 m*M* sodium phosphate, pH 7.2) was used.

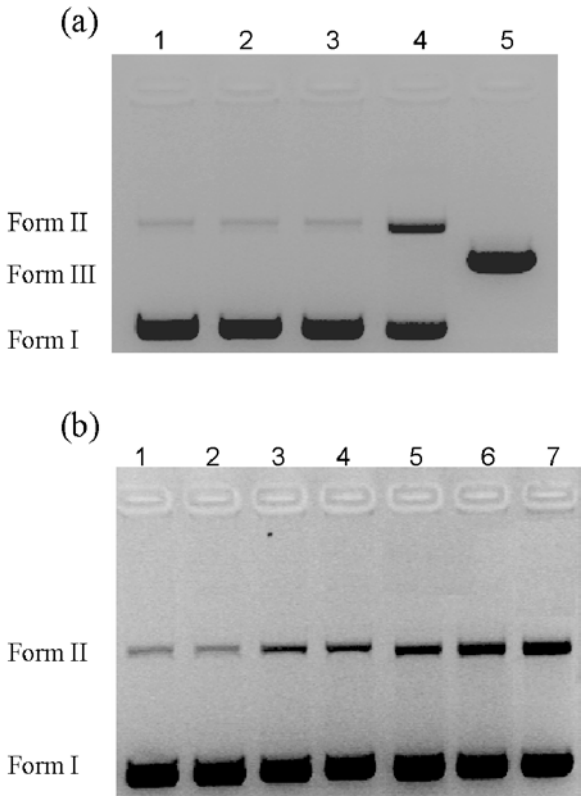

Figure 4. EtBr-stained agarose gel (2%) showing the photocleavage of 120 μ*M* pUC19 plasmid by 30 μ*M* DAP after 30 min incubation and 30 min of irradiation in 10 m*M* phosphate buffer, pH = 7.5. a: Lane 1, plasmid only, dark; Lane 2, plasmid only, irradiated; Lane 3, plasmid + DAP, dark; Lane 4, plasmid + DAP, irradiated; Lane 5, plasmid + *Eco*R1 restriction enzyme. b: Lane 1, plasmid only, dark; Lane 2, plasmid only, irradiated; Lanes 3–7, plasmid + DAP photolyzed with visible light for 30 min with Lane 3, pH = 4.0; Lane 4, pH = 5.0; Lane 5, pH = 6.0; Lane 6, pH = 7.0 and Lane 7, pH = 8.0.

pH = 7.5), an emission enhancement is observed. Luminescence enhancement is often observed with emissive intercalators. Enhanced luminescence can result from π-stacking interaction with the DNA bases and protection of the intercalator from aqueous environment. The emission enhancement of DAP upon binding to DNA is consistent with intercalation (54–59). Although, a competitive binding study with EtBr can be undertaken to confirm intercalation (52,53,60,61), the large difference in binding constant between DAP and EtBr ($\sim 5 \times 10^5\ M^{-1}$) precludes the use of this technique for this particular system (51,52). However, the observed emission enhancement of DAP upon DNA binding is consistent with protection of the molecule from the surrounding water, which is typical of molecules that intercalate between the bases (54,55,58,59). It has been reported that DAP has a more intense fluorescence in nonpolar solvents, such as acetone and diethyl ether, than in water, a difference attributed to its use of water as a source of protons (6,34,42–44).

Changes in relative viscosity provide a reliable method for the assignment of DNA binding modes by intercalators and groove binders (56,57). The changes in the relative viscosity of solutions containing 2.5 m*M* herring sperm DNA upon addition of increasing concentrations of DAP are shown in Fig. 3b and parallel those observed for the intercalator EtBr. In contrast, addition of the minor groove binder Hoechst 33258 does not result in significant changes in the relative viscosity (56,57), which is typical for minor groove and electrostatic binders that do not intercalate between the DNA bases (29,31–33,54–57,60,61). The viscosity data taken together with the hypochromic shift and luminescence enhancement upon addition of DNA are in accord with an intercalative binding mode for DAP. The slope from the EtBr data (~0.91) in Fig. 3b is very close to that predicted for an ideal intercalator, 1.0 (58). In contrast, the slope observed for DAP is ~0.57, which can be explained by its low binding constant to DNA. It is also possible that DAP has other binding modes to ds-DNA in addition to intercalation, such as hydrogen bonding through the two amino groups. A slope significantly lower than 1.0 in the viscosity changes as a function of additive concentration has been related previously to multiple binding modes, one of which is intercalation (30,59).

DNA photocleavage

The image of the EtBr-stained gel in Fig. 4a shows the DNA photocleavage of 120 μ*M* pUC19 plasmid by DAP. The control lanes show that irradiation of the plasmid (pUC19) alone with visible light for 5 J/cm^2 does not result in DNA damage (Lanes 1 and 2). In addition to the supercoiled plasmid (Form I), a small amount of circular (nicked, Form II) is also found in the control lanes.

Linearization of the pUC19 supercoiled plasmid with the *Eco*R1 restriction enzyme results in the exclusive formation of cut, linear (Form III) ds-DNA, as shown in Lane 5 (Fig. 4a). As shown in Fig. 4a, the addition of 30 μ*M* DAP to 120 μ*M* pUC19 plasmid does not result in cleavage in the dark (Lane 3); however, irradiation of the mixture for 5 J/cm^2 with visible light (λ_{irr} = 400–700 nm, 30 min) results in the formation of nicked ds-DNA (Lane 4, Form II).

Because the protonation and deprotonation states of the DAP have been shown to have a profound effect on the excited-state properties, the efficiency of DNA cleavage upon irradiation was measured as a function of pH (Fig. 4b). As shown in Fig. 4b, in the pH range from 3.0 to 8.0, irradiation of 120 μ*M* pUC19 plasmid in the presence of 30 μ*M* DAP with visible light results in the formation of ~28% nicked plasmid at pH 8. A marked decrease in nicked DNA is evident with the decrease of the pH from 8.0 to 4.0 (Fig. 4b). The results are consistent with greater DNA photocleavage sensitized by DAP in its deprotonated state, where greater reactivity is observed at pH values of 7 and 8, and a marked decrease in cleavage is evident with the decrease of the solution pH from 6 to 4. It is important to note that because of the weak interaction between DAP and ds-DNA, a 30 min incubation before irradiation is needed for any DNA photocleavage to occur.

DAP exhibits DNA photophysical and photobiological characteristics similar to many fluorescent DNA dyes regardless of its weak binding constant with ds-DNA. It has been demonstrated that many photoactive DNA dyes are able to intercalate between nucleobases and nick plasmid DNA in the presence of molecular oxygen and visible light (62–65). The search for molecules with desirable photophysical properties, which can function as efficient artificial photonucleases and biomolecular probes, has resulted in the discovery of a large number of DNA intercalators that can cleave ds-DNA via photochemical pathways (66–72). Even though DAP has proven to possess interesting photosensitizing characteristics upon irradiation with visible light, it is important to determine whether it has any functional role in biological systems.

Photocytotoxicity

Irradiation of human skin fibroblasts (Hs-27) exposed to 5–25 μ*M* DAP with 400–700 nm light for 30 min (5 J/cm^2) results in the death of 25–83% of the cells, respectively, as shown in Fig. 5. In contrast, >95% cell survival was observed in solutions containing similar DAP concentrations that were not irradiated with visible light (Fig. 5). Without irradiation, the survival rate of Hs-27 at concentrations of DAP up to 125 μ*M* was ~65%.

There is a striking difference in potency between the photocytotoxicity and cytotoxicity of DAP toward Hs-27 cells. The concentration of DAP, which results in 50% cell death, the lethal concentration 50 (LC_{50}), for cultures in the dark and exposed to visible light was found to be 172 and 13 μ*M*, respectively. These results clearly show that in addition to the toxicity reported previously for DAP in the dark; the dye is a potent photosensitizer whose cytotoxicity increases by a factor of 13 upon exposure to visible light. Therefore, cells simultaneously exposed to DAP and visible light, the major component of natural sunlight, may be subject to significant cellular damage.

CONCLUSIONS

The ground-state absorption and excited-state emission of DAP are pH dependent. The molecule fluoresces strongly in its deprotonated form (pH = 8), and the emission intensity decreases by an order of magnitude at pH = 3. Enhancement of the emission and the increase in viscosity upon binding of DAP to ds-DNA establishes that this molecule intercalates between the bases in DNA with a binding constant of 3.5 × 10^3 M^{-1}. However, the changes in relative viscosity point at multiple binding modes, one of which is intercalation. Furthermore, DAP is able to produce single-strand nicks in plasmid DNA upon irradiation with visible light. The cytotoxicity of DAP toward human skin fibroblasts (Hs-27) was evaluated both in the dark and upon exposure of the cell cultures with various concentrations of DAP to visible light. It was observed that DAP increases the sensitivity of human skin fibroblasts toward visible light by a factor of 13, resulting in LC_{50} values of 172 and 13 μ*M* in the dark and upon irradiation, respectively. The excited-state intermediates responsible for the photocytotoxicity of DAP remain unknown; however, preliminary experiments show that sodium azide, a known scavenger of singlet oxygen, results in the complete inhibition of the DNA photocleavage by DAP (supplementary material). It is well known that intercalator aromatic amines usually cleave DNA through the generation of reactive oxygen species (67,70–73). The potential presence of DAP as a contaminant in consumer products and with subsequent topical human exposure on sun-exposed skin requires further investigation of its harmful effects and photodamage to human cells.

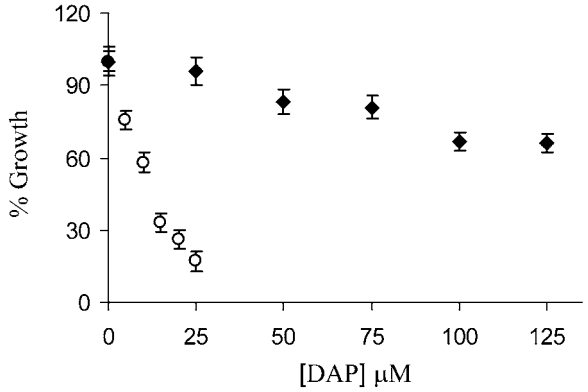

Figure 5. Toxicity tests of DAP. Human skin fibroblasts were incubated in the dark (cytotoxicity, ◆) or irradiated (photocytotoxicity, ○) with various concentrations of DAP for 30 min. Cell cultures were irradiated with visible light (400–700 nm) with the light intensity of 5 J/cm^2. Interpolation of the data points was used to determine the concentration of DAP required to achieve 50% cell death, LC_{50}. Each point represents the mean of four determinations and ±5% error.

Acknowledgements—C.T. thanks the National Institutes of Health (RO1 GM64040-01) for their generous support, and P.K.F. thanks the Office of Cosmetic and Colors, Center for Food and Applied Nutrition, FDA for their support of this study.

REFERENCES

1. Watanabe, T., T. Hirayama and S. Fukui (1990) Mutagenicity of commercial hair dyes and detection of 2,7-diaminophenazine. *Mutat. Res.* **244**, 303–308.
2. Wagner, E. D., A. Cebulska-Wasilewska, S. Connolly and M. J. Plewa (1996) Mutagenic analysis of 2,3-diaminophenazine and 2-amino-3-hydroxyphenazine in Salmonella strains expressing different levels of o-acetyltransferase with and without plant and mammalian activation. *Mutat. Res.* **372**, 65–74.

3. Køppe, B. (1992) Liquid chromatographic determination of 2-hydroxy-3- aminophenazine and 2,3-diaminophenazine as impurities in pesticide formulations containing benomyl or carbendazim. *J. Chromatogr. A,* **623**(1), 168–173.
4. Sarrif, A. M., G. T. Arce, D. F. Krahn, R. M. O'Neil and V. L. Reynolds (1994) Evaluation of carbendazim for gene mutations in the Salmonella/Ames plate-incorporation assay: the role of aminophenazine impurities. *Mutat. Res./Gene. Tox.* **321**, 43–56.
5. Sun, W., K. Jiao and S. S. Zhang (2001) Electrochemical ELISA for the detection of cucumber mosaic virus using o-phenylenediamine as substrate. *Talanta* **55**, 1211–1218.
6. Mekler, V. M. and S. M. Bystryak (1992) Application of o-phenylenediamine as fluorogenic substance in peroxidase-mediated enzyme-linked immunosorbent assay. *Anal. Chim. Acta* **264**, 359–363.
7. Hamilton, T. M., A. A. Dobie-Galuska and S. M. Wietstock (1999) The o-phenylenediamine horseradish peroxidase system: enzyme kinetics in the gereral chemistry laboratory. *J. Chem. Edu.* **76**, 642–647.
8. Rosso, N. D., B. Szpoganicz and A. E. Martell (1999) Catalytic oxidation of 1,2-diaminobenzene by the dinuclear cobalt(II)-obisdien dioxygen complex. *Inorg. Chim. Acta* **287**, 193–198.
9. Tanner, A., L. Bowater, A. S. Fairhurst and S. Bornemann (2001) Oxalate decarboxylase requires manganese and dioxygen for activity. *J. Biol. Chem.* **276**, 43627–43634.
10. Zuyun, H., H. Huang, R. Cai and Y. Zeng (1998) Organic solvent enhanced spectrofluorimetric method for determination of lactase activity. *Anal. Chim. Acta* **374**, 99–103.
11. Zhang, K., R. Cai, D. Chen and L. Mao (2000) Determination of hemoglobin based on its enzymatic activity for the oxidation of o-phenylenediamine with hydrogen peroxide. *Anal. Chim. Acta* **413**, 109–113.
12. Watanabe, T., T. Hirayama and S. Fukui (1989) Phenazine derivatives as the mutagenic reaction product from o- or m-phenylenediamine derivatives with hydrogen peroxide. *Mutat. Res.* **227**, 135–145.
13. Cebulska-Wasilewska, A., D. Nowak, W. Niedzwiedz, E. D. Wagner and M. J. Plewa (1999) Studies on the genotoxic effects of aminophenazines using two cellular models and three different methods. *Mutat. Res.* **446**, 57–65.
14. Cebulska-Wasilewska, A., D. Nowak, D. Niedzwiedz and D. Anderson (1998) Correlation between DNA and cytogenetic damage induced after chemical treatment and radiation. *Mutat. Res.* **421**, 83–91.
15. Watanabe, T., T. Kasai, M. Arima, K. Okumura, N. Kawabe and T. Hirayama (1996) Genotoxicity *in vivo* of phenazine and aminophenazines assayed in the wing spot test and the DNA-repair test *Drosophila melanogaster*. *Mutat. Res.* **369**, 75–80.
16. Thomas, K. A. and W. B. Euler (2001) An electrochemical spectroscopic, and theoretical study of poly(2,3-diaminophenazine). *J. Electroanal. Chem.* **501**, 235–240.
17. Mekler, V. M. and S. M. Bystryak (1992) Autosensitized oxidation of o-phenylenediamine in an aqueous buffer solution. *J. Photochem. Photobiol. A: Chem.* **65**, 391–397.
18. Bystryak, S. M. and V. M. Mekler (1992) Photochemical amplification for horseradish peroxidase-mediated immunosorbent assay. *Anal. Biochem.* **202**, 309–393.
19. Mekler, V. M., O. V. Belonogova and V. I. Nikulin (1995) Photochemical mimetics of chromogenic catalymetric reactions of arylamines in water solutions. *J. Photochem. Photobiol. A: Chem.* **87**, 243–247.
20. Doyle, R. P., P. E. Kruger, P. R. Mackie and M. Nieuwenhuyzen (2001) Phenazine-2,3-diamine. *Acta Crystallogr. C.* **57**, 104–105.
21. Zang, K., L. Y. Mai and R. X. Cai (2000) Stopped-flow spectrophotometric determination of hydrogen peroxide with hemoglobin as catalyst. *Talanta* **51**, 179–186.
22. Yuan, H., R. Cai and Z. Pan (2003) Catalitical kinetic determination of hydrogen peroxide using iron-tetrasulfonatophthalocyanine (with r-CD) as a mimetic enzyme of peroxidase. *Anal. Lett.* **36**, 277–286.
23. Jang, D.-H., Y.-S. Yoo and S. M. Oh (1995) Electropolymerization mechanism for poly(o-phenylenediamine) (PPD) and its electrocatalytic behavior for O_2 reduction. *Bull. Korean Chem. Soc.* **16**, 392–397.
24. Sambrook, J. and D. W. Russel (2001) *Molecular Cloning, A Laboratory Manual.* Cold Spring Harbor Laboratory Press, Cold Spring Harbor, New York.
25. Baruah, H. and U. Bierbach (2003) Unusual intercalation of acridin-9-ylthiourea into the 5′-GA/TC DNA base step from the minor groove: implications for the covalent DNA adduct profile of a novel platinum-intercalator conjugate. *Nucleic Acids Res.* **31**, 4138–4146.
26. Ren, J. and J. B. Chaires (1999) Sequence and structural selectivity of nucleic acid binding ligands. *Biochemistry* **38**, 16067–16075.
27. Chaires, J. B., J. Ren, M. Henary, O. Zegrocka, G. R. Bishop and L. Strekowski (2003) Triplex selective 2-(2-naphthyl)quinoline compounds: origins of affinity and new design principles. *J. Am. Chem. Soc.* **125**, 7272–7283.
28. Schmechel, D. E. and D. M. Crothers (1971) Kinetic and hydrodynamic studies of the complex of proflavine with poly A-poly U. *Biopolymers* **10**, 465–480.
29. Wolfe A., G. H. Shimer Jr. and T. Meehan (1987) Polycyclic aromatic hydrocarbons physically intercalate into duplex regions of denatured DNA. *Biochemistry* **26**, 6392–6396.
30. Luedtke, N. W., J. S. Hwang, E. Nava, D. Gut, M. Kol and Y. Tor (2003) The DNA and RNA specificity of eilatin Ru(II) complexes as compared to eilatin and ethidium bromide. *Nucleic Acid Res.* **31**, 5732–5740.
31. Satyanarayana, S., J. C. Dabrowiak and J. B. Chaires (1992) Neither Δ- nor Λ-tris (phenanthroline) ruthenium binds to DNA by classical intercalation. *Biochemistry* **31**, 9319–9324.
32. Satyanarayana, S., J. C. Dabrowiak and J. B. Chaires (1993) Tris (phenanthroline) ruthenium (II) enantiomer interaction with DNA: mode and specificity of binding. *Biochemistry* **32**, 2573–2584.
33. Scaria, P. V. and R. H. Shafer (1991) Binding of ethidium bromide to a DNA triple helix. *J. Biol. Chem.* **266**, 5417–5423.
34. Brown, K. C., J. F. Corbett and N. P. Loveless (1979) Spectrophotometric studies on the protonation of hydroxyl and aminophenazines in aqueous solution. *Spectrochim. Acta Part A* **35**, 421–423.
35. Pileni, M.-P. and M. Gratzel (1980) Light induced redox reaction of proflavin in aqueous and micellar solution. *J. Phys. Chem.* **84**, 2402–2406.
36. Gesan, V. and R. Ramaraj (2001) Spectral properties of proflavin in zeolite-L and zeolite-Y. *J. Lumin.* **92**, 167–173.
37. Gabor, G., C. Suneet and D. R. Walt (1995) Sensitivity enhancement of fluorescent pH indicators using pH-dependent energy transfer. *Anal. Chim. Acta* **313**, 131–137.
38. Teuber, M., M. Rogner and S. Berry (2001) Fluorescent probes for non-invasive bioenergetic studies of whole cyanobacterial cells. *Biochim. Biophys. Acta* **1506**, 31–46.
39. Gangola, P., N. B. Joshi and D. D. Pant (1979) Edge excitation red-shift and excited-state proton association in acridine. *Chem. Phys. Lett.* **60**, 329–331.
40. Sharma, V. K., P. D. Sahare, R. C. Rastogi, S. K. Ghoshal and D. Mohan (2003) Excited state characteristics of acridine dyes; acriflavin and acridine orange. *Spectrochim. Acta Part A* **59**, 1799–1804.
41. Choudhury, S. D. and S. Basu (2003) Singlet state exciplet formation of phenazine with some aromatic amines. *Chem. Phys. Lett.* **373**, 67–71.
42. del Barrio, J. I., J. R. Rebato and F. M. G. Tablas (1989) Basicity of phenazine in the first triplet state. *J. Phys. Chem.* **93**, 6836–6837.
43. Chalvet, O., H. H. Jaffe and J. C. Rayez (1977) Acid-base equilibria of electronically excited phenazine. *Photochem. Photobiol.* **26**, 353–356.
44. Aaron, J. J. and M. Maafi (1995) Quantitative treatment of the solvent effects on the electronic absorption and fluorescence spectra of acridines and phenazines. The ground and first excited singlet-state dipole moments. *Spectrochim. Acta Part A* **51**, 603–615.
45. Dietrich, B., R. Ghahary and H. Pasch (1996) Triazine-based polymers. 4. MALDI-MS of triazine-based polyamines. *Polymer* **37**, 777–783.
46. Poulios, I., D. Sazou and G. Kokkinidis (1988) Photoelectrochemical behavior of electrogenerated poly(2,3-diaminophenazine) on platinum in aqueous media. *Synth. Metals* **26**, 339–347.
47. Crank, G. and M. I. H. Makin (1989) Photochemical conversion of o-phenylenediamine and o-aminophenol into heterocyclics. *J. Heterocyclic Chem.* **26**, 1163–1166.
48. Fu, K.-L. P. and C. Turro (2001) Transcription inhibition and DNA photocleavage by metal complexes. Doctoral thesis, The Ohio State University, Columbus, OH.
49. Fu, K.-L. P., P. M. Bradley and C. Turro (2003) Stabilization of duplex DNA structure and suppression of transcription in vitro by bis(quinone diimine) complexes of rhodium(III) and ruthenium(II). *Inorg. Chem.* **42**, 878–884.
50. Sorasaenee, K., P. K.-L. Fu, A. M. Angeles-Boza, K. R. Dunbar and C. Turro (2003) Inhibition of transcription in vitro by anticancer active dirhodium(II) complexes. *Inorg. Chem.* **42**, 1267–1271.
51. Billadeau, M. A. and H. Morrison (1995) Photoaquation of cis-Dichlorobis-(1,10-phenanthroline) chromium (III) and the photochemical

and thermal reactions of this complex with native calf-thymus DNA. *J. Inorg. Biochem.* **57**, 249–270.
52. Rosu, F., E. D. Pauw, L. Guittat, P. Alberti, L. Lacroix, P. Mailliet, J.-F. Riou and J.-L. Mergny (2003) Selective interaction of ethidium derivatives with quadruplexes: an equilibrium dialysis and electrospray ionization mass spectrometry analysis. *Biochemistry* **42**, 10361–10371.
53. Qu, X. and J. B. Chaires (2001) Hydration changes for DNA intercalation reactions. *J. Am. Chem. Soc.* **123**, 1–7.
54. Vaidyanathan, V. G. and B. U. Nair (2003) Synthesis, characterization and binding studies of chromium (III) complex containing an intercalating ligand with DNA. *J. Inorg. Biochem.* **95**, 334–342.
55. Hiort, C., P. Lincoln and B. Norden (1993) DNA-binding of Δ- and Λ-$[Ru(phen)_2DPPZ]^{2+}$. *J. Am. Chem. Soc.* **115**, 3448–3454.
56. Suh, D., Y.-K. Oh and J. B. Chaires (2001) Determining the binding mode of DNA sequence specific compounds. *Process Biochem.* **37**, 521–525.
57. Haq, I., P. Lincoln, D. Suh, B. Norden, B. Z. Chowdhry and J. B. Chaires (1995) Interaction of DELTA—and LAMBDA $[Ru(phen)_2DPPZ]^{2+}$ with DNA: a calorimetric and equilibrium binding study. *J. Am. Chem. Soc.* **117**, 4788–4796.
58. Cohen, G. and H. Eisenbrg (1969) Viscosity and sedimentation study of sonicated DNA-proflavin complexes. *Biopolymers* **8**, 45–55.
59. Jin, E., V. Katritch, W. K. Olson, M. Kharatisvil, R. Abagyan and D. S. Pilch (2000) Aminoglycoside binding in the major groove of duplex RNA: the thermodynamic and the electrostatic forces that govern recognition. *J. Mol. Biol.* **298**, 95–110.
60. Tang, T. C. and H. J. Huang (1999) Electrochemical studies of the intercalation of ethidium bromide to DNA. *Electroanalysis.* **11**, 1185–1190.
61. Xie, H. P., J. H. Jiang, X. Chu, H. Cui, H. L. Wu, G. L. Shen and R. Q. Yu (2002) Competitive interaction of the antitumor drug daunorubicin and the fluorescence probe ethidium bromide with DNA as studied by resolving trilinear fluorescence data: the use of PARAFAC and its modification. *Anal. Bioanal. Chem.* **373**, 159–162.
62. Jennette, K. W., S. J. Lippard, G. A. Vassiliades and W. R. Bauer (1774) Metallointercalation reagents 2-hydroxyethanethiolato(2,2′,2′-terpyridine)-platinum(II) monocation binds strongly to DNA by intercalation. *Proc. Natl. Acad. Sci. USA* **71**, 2829–2843.
63. Cosa, G., K.-S. Focsaneanu, J. R. N. McLean and J. C. Scaiano (2000) Direct determination of single to double stranded DNA in solution applying time-resolved fluorescence measurement of dye-DNA complexes. *Chem. Commun.* **8**, 689–690.
64. Cosa, G., K.-S. Focsaneanu, J. R. N. McLean, J. P. McNamee and J. C. Scaiano (2002) Photophysical properties of fluorescent DNA-dyes bound to single- and double-stranded DNA in aqueous buffered solution. *Photochem. Photobiol.* **73**, 585–619.
65. Birnboim H. C. and J. J. Jevcak (1981) Fluorimetric method for rapid detection of DNA strand breaks in human white blood cells produced by low doses of radiation. *Cancer Res.* **41**, 1889–1892.
66. Rogers, K. R., A. Apostol, S. J. Madsen and C. W. Spencer (1999) Detection of low dose radiation induced DNA damage using temperature differential fluorescence assay. *Anal. Chem.* **71**, 4423–4426.
67. Steullet, V., S. Edwards-Bennett and D. W. Dixon (1999) Cleavage of abasic sites in DNA by intercalator-amines. *Bioorg. Med. Chem.* **7**, 2531–2540.
68. Fernandez-Saiz, M., P. T. Henderson, W. D. Wilson and G. B. Schuster (1999) Selective photocleavage of DNA and RNA by anthraquinone derivatives: targeting the single-strand region of hairpin structures. *Photochem. Photobiol.* **70**, 847–852.
69. Reynisson, J., G. B. Schuster, S. B Howerton, L. D. Williams, R. N. Barnett, C. L. Cleveland, U. Landman, N. Harrit and J. B. Chaires (2003) Intercalation of trioxatriangulenium ion in DNA: binding, electron transfer, x-ray crystallography, and electronic structure. *J. Am. Chem. Soc.* **26**, 2072–2083.
70. Turro, C., D. B. Hall, W. Chen, H. Zuilholf, J. K. Barton and N. J. Turro (1998) Photoreactivity of phenanthrenequinone diimine complexes of rhodium and correlations with DNA photocleavage and photooxidation. *J. Phys. Chem. A* **102**, 5708–5715.
71. Delaney, S., M. Pascaly, P. K. Bhattacharya, K. Han and J. K. Barton (2002) Oxidative damage by ruthenium complexes containing the dipyridophenazine ligand or its derivatives: a focus on intercalation. *Inorg. Chem.* **41**, 1966–1974.
72. Copeland, K. D., A. M. Lueras, E. D. Stemp and J. K. Barton (2002) DNA cross-linking with metallointercalator-peptide conjugates. *Biochemistry* **22**, 12785–12797.
73. Kornhauser, A., W. G. Wamer and L. A. Lambert (2002) Cellular and molecular events following ultraviolet irradiation of skin. In *Dermatotoxicology* (Edited by F. N. Marzulli and H. I. Maibach), pp. 189–230. Taylor & Francis, Washington, DC.